Available online at www.sciencedirect.com
ScienceDirect
Journal of Computational Physics 226 (2007) 1–16
JOURNAL OF COMPUTATIONAL PHYSICS
www.elsevier.com/locate/jcp

Short Note

A note on hybrid Eulerian/Lagrangian computation of compressible inviscid and viscous flows ☆

Bo Gao, Shan-Shu Xu, Zi-Niu Wu *

Department of Engineering Mechanics, Tsinghua University, Beijing 100084, PR China

Received 27 September 2006; received in revised form 21 May 2007; accepted 29 May 2007
Available online 8 June 2007

Keywords: Eulerian coordinates; Lagrangian coordinates; Hybrid approach; Compressible flow; Viscous flow

1. Introduction

There are two classical coordinate systems used to describe fluid flows: the Eulerian coordinate system and the Lagrangian coordinate system. In the Eulerian approach, one considers what happens at every fixed point in space as a function of time. The velocities and the other properties of fluid elements are considered to be functions of time and fixed space coordinates. In the Lagrangian approach, one looks for the dynamic history of each selected fluid element. The positions of fluid particles and the other properties are considered to be functions of the time and their initial positions.

The Eulerian approach is simple to use because it uses fixed grid. It is very efficient to treat viscous flows with boundary layers or with geometry singularity. However, the fact that fluid particles move across cell interfaces may cause excessive numerical diffusion in the numerical solutions. Indeed, slip lines are smeared badly and shocks are also smeared.

The Lagrangian approach is well suited to problems with slip lines. There is no convective flux across cell interfaces and numerical diffusion is minimized. However, the moving cells, exactly following fluid particles, could result in severe grid deformation, causing inaccuracy and even breakdown of the computation. Though a unified coordinate system was introduced by Hui et al. [7,8] which combines the advantages of the Eulerian approach and the Lagrangian approach. It still has some difficulty in treating the flow near the wall if there is singularity or if there is a boundary layer [9].

In this note, we propose an approach using hybrid Eulerian/Lagrangian coordinates to compute compressible flows, with geometry singularity or with boundary layers for which a pure Lagrangian approach has some difficulty. The Eulerian domain is close to the wall while the Lagrangian domain is elsewhere. The two subdomains have an overlapping region at their interface and data interpolation is used to match the solutions

☆ This work was supported by the research fund of Laboratory of Computational Physics of IAPCM and by Chinese National Natural Science Foundations (Contract No. 10376016).
* Corresponding author.
E-mail address: ziniuwu@tsinghua.edu.cn (Z.-N. Wu).

0021-9991/$ - see front matter
doi:10.1016/j.jcp.2007.05.019

between the two subdomains. In the Lagrangian subdomain, we use the unified coordinate system to avoid severe grid deformation.

Hybrid Eulerian/Lagrangian approaches are found for incompressible flow or mixed compressible/incompressible flow. For instance, a domain decomposition technique was proposed in [1,2] where a Lagrangian vortex method and an Eulerian approach are combined to simulation 2D external incompressible viscous flows. The Eulerian domain is near the solid boundary, where viscous effects are important and the Lagrangian domain is far from the solid boundary, where convection is important. A hybrid Lagrangian/Eulerian method for the vortex methods has also been proposed, see [3]. A ghost fluid method (GFM) was also proposed in [4–6] which addresses multi-phase multi-fluid problems using a hybrid approach. Using a hybrid Eulerian/Lagrangian approach to treat compressible flows with shock waves, slip lines and boundary layers or singularities seems to be new.

In the following we first outline the hybrid approach, then we give several examples to demonstrate the behavior of the hybrid approach.

2. Hybrid approach

2.1. Equations on the Eulerian and Lagrangian coordinates

The Navier–Stokes equations in the Eulerian domain are

$$\frac{\partial \mathrm{w}}{\partial \mathrm{t}}+\frac{\partial \mathrm{f}(\mathrm{w})}{\partial \mathrm{x}}+\frac{\partial \mathrm{g}(\mathrm{w})}{\partial \mathrm{y}}=\frac{\partial \mathrm{f}^{(\mathrm{V})}(\mathrm{w})}{\partial \mathrm{x}}+\frac{\partial \mathrm{g}^{(\mathrm{V})}(\mathrm{w})}{\partial \mathrm{y}}, \tag{1}$$

where

$$\mathrm{w}=\begin{pmatrix}\rho\\ \rho\mathrm{u}\\ \rho\mathrm{v}\\ \rho\mathrm{e}\end{pmatrix},\quad \mathrm{f}(\mathrm{w})=\begin{pmatrix}\rho\mathrm{u}\\ \rho\mathrm{u}^2+\mathrm{p}\\ \rho\mathrm{uv}\\ \rho\mathrm{ue}\end{pmatrix},\quad \mathrm{g}=\begin{pmatrix}\rho\mathrm{v}\\ \rho\mathrm{vu}\\ \rho\mathrm{v}^2+\mathrm{p}\\ \rho\mathrm{ve}\end{pmatrix},$$

$$\mathrm{f}^{(\mathrm{V})}(\mathrm{w})=\begin{pmatrix}0\\ \tau_{\mathrm{xx}}\\ \tau_{\mathrm{xy}}\\ \mathrm{u}\tau_{\mathrm{xx}}+\mathrm{v}\tau_{\mathrm{xy}}-\chi_{\mathrm{x}}\end{pmatrix},\quad \mathrm{g}^{(\mathrm{V})}(\mathrm{w})=\begin{pmatrix}0\\ \tau_{\mathrm{yx}}\\ \tau_{\mathrm{yy}}\\ \mathrm{u}\tau_{\mathrm{yx}}+\mathrm{v}\tau_{\mathrm{yy}}-\chi_{\mathrm{y}}\end{pmatrix}.$$

Here u and v are the x-and y-component of fluid velocity and ρ, p and e with $\mathrm{e}=\frac{1}{2}(\mathrm{u}^2+\mathrm{v}^2)+\frac{1}{\gamma-1}\frac{\mathrm{p}}{\rho}$ are the density, pressure and specific total energy of the gas, τ_{xx}, τ_{xy}, τ_{yx} and τ_{yy} are viscous stresses, whose exact formulas can be found in any text book of fluid mechanics, χ_x and χ_y are heat flux components.

The Navier–Stokes equations in the Lagrangian domain, using unified coordinates, are [7,8]

$$\frac{\partial \mathrm{E}}{\partial \lambda}+\frac{\partial \mathrm{F}}{\partial \xi}+\frac{\partial \mathrm{G}}{\partial \eta}=\frac{\partial \mathrm{F}^{(\mathrm{V})}}{\partial \xi}+\frac{\partial \mathrm{G}^{(\mathrm{V})}}{\partial \eta}, \tag{2}$$

where $E=(\rho\Delta,\rho\Delta u,\rho\Delta v,\rho\Delta e,A,B,L,M)^{\mathrm{t}}$, $F^{(\mathrm{V})}=\Delta(\xi_x f^{(\mathrm{V})}+\xi_y g^{(\mathrm{V})})$, $G^{(\mathrm{V})}=\Delta(\eta_x f^{(\mathrm{V})}+\eta_y g^{(\mathrm{V})})$ and

$$\mathrm{F}=\begin{pmatrix}\Delta(\xi_{\mathrm{t}}\mathrm{w}+\xi_{\mathrm{x}}\mathrm{f}(\mathrm{w})+\xi_{\mathrm{y}}\mathrm{g}(\mathrm{w}))\\ -\mathrm{hu}\\ -\mathrm{hv}\\ 0\\ 0\end{pmatrix},\quad \mathrm{G}=\begin{pmatrix}\Delta(\eta_{\mathrm{t}}\mathrm{w}+\eta_{\mathrm{x}}\mathrm{f}(\mathrm{w})+\eta_{\mathrm{y}}\mathrm{g}(\mathrm{w}))\\ 0\\ 0\\ -\mathrm{hu}\\ -\mathrm{hv}\end{pmatrix}$$

with $\Delta=AM-BL=x_\xi y_\eta-x_\eta y_\xi$. Here, the unified coordinates (λ,ξ,η) are related to the Eulerian coordinates by

$$\begin{aligned} dt &= d\lambda, \\ dx &= hu\,d\lambda + A\,d\xi + L\,d\eta = x_\lambda\,d\lambda + x_\xi\,d\xi + x_\eta\,d\eta, \\ dy &= hv\,d\lambda + B\,d\xi + M\,d\eta = y_\lambda\,d\lambda + y_\xi\,d\xi + y_\eta\,d\eta. \end{aligned} \tag{3}$$

The unified coordinates move with velocity hq, q being the velocity vector. h is a free function introduced by the unified coordinate system. It includes the Eulerian coordinates as special case when $h = 0$ and the Lagrangian coordinates when $h = 1$. An equation for h controlling the quality of the grid is simultaneously solved. The angle-preserving h-equation in the UCS subdomain is given by

$$\begin{aligned} &S^2(A\sin\theta - B\cos\theta)\frac{\partial \ln(hq)}{\partial\xi} + T^2(M\cos\theta - L\sin\theta)\frac{\partial \ln(hq)}{\partial\eta} \\ &\quad = S^2\left(B\frac{\partial\cos\theta}{\partial\xi} - A\frac{\partial\sin\theta}{\partial\xi}\right) - T^2\left(M\frac{\partial\cos\theta}{\partial\eta} - L\frac{\partial\sin\theta}{\partial\eta}\right), \end{aligned} \tag{4}$$

where $q = \sqrt{u^2 + v^2}, S^2 = L^2 + M^2, T^2 = A^2 + B^2$ and θ is the flow angle: $u = q\cos\theta$, $v = q\sin\theta$. For more details, see Hui et al. [7,8].

In using the Eulerian coordinates the computational cells are fixed in space, while fluid particles move across cell interfaces. This convective flux may cause excessive numerical diffusion in the numerical solutions. As a result, shock waves and slip lines are smeared.

In using the unified coordinates, we can avoid excessive numerical diffusion across slip lines in the Eulerian coordinates and avoid severe grid deformation in the Lagrangian coordinates, yet it retains sharp resolution of slip lines, especially for steady flows.

However, the unified coordinate system has some disadvantages. For inviscid flows, the boundary cells glide along the wall. If the wall contains singular points, the boundary of the computational domain cannot coincide with the physical boundary and the singular grid point cannot be fixed in the grid system (see Fig. 1). As a result, the geometry near singular points could not be well captured, leading to inaccurate solutions.

On the other hand, for viscous flow, the velocity of fluid particles q vanishes on the wall. This causes severe grid deformation as in Lagrangian coordinates. Moreover, the vertical components of the velocity would make the grid to get sparse (see Fig. 2) so that the boundary layer cannot be well resolved. See [9] for more details.

2.2. Hybrid interface

In the hybrid method we propose, the entire flow domain is decomposed into a Eulerian subdomain that is attached to the wall and a Lagrangian subdomain that covers the rest of the domain. The adjacent Eulerian and Lagrangian subdomains have an overlap (see Fig. 3).

In the course of computation, the grid in the Lagrangian subdomain moves at each time step (the motionless viewing window technique is applied, see [7]), as illustrated in Fig. 3 where the grids in two subsequent

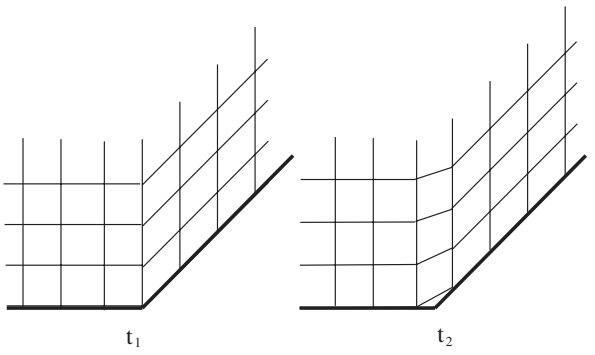

Fig. 1. Lagrangian grids around a singularity at two different instants. The boundary of the computational domain cannot coincide with the physical boundary.

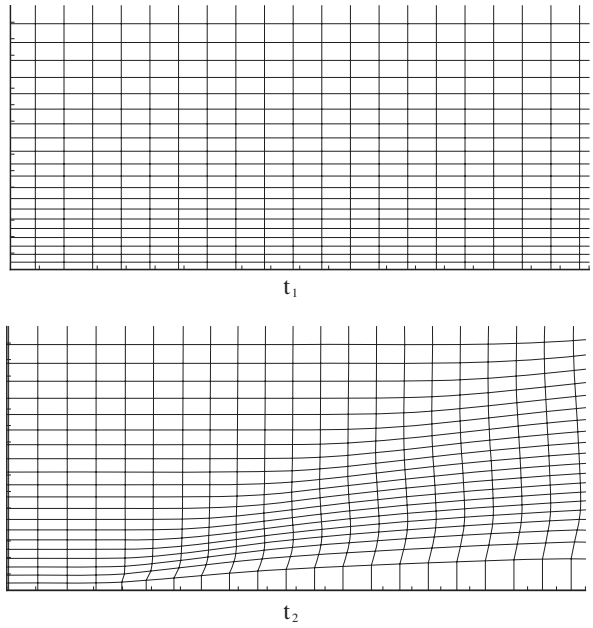

Fig. 2. Lagrangian grids inside the boundary layer at two different instants. The vertical components of the velocity would make the grid to get sparse.

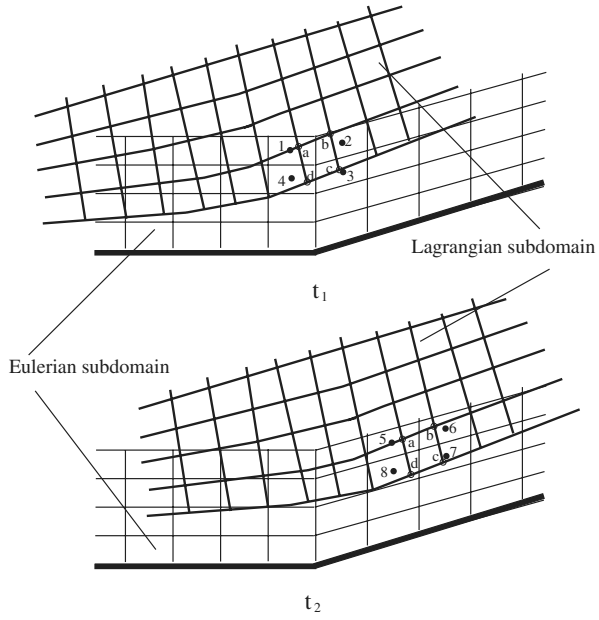

Fig. 3. Hybrid Euler/Lagrangian grid. One boundary cell "*abcd*" of the Lagrangian subdomain lies between the interior cells "1", "2", "3" and "4" of the Eulerian subdomain at t_1 and lies between the interior cells "5", "6", "7" and "8" of the Eulerian subdomain at t_2.

instants are given. Hence, the location of the boundary cells at the interface must be decided at each time step. Consider for instance the boundary cell "*abcd*" of the Lagrangian subdomain. At instant t_1, it lies between the interior cells "1", "2", "3" and "4" of the Eulerian subdomain. At instant t_2, it lies between the interior cells "5", "6", "7" and "8" of the Eulerian subdomain. Due to the limitation of numerical stability, the grid moves a distance far less than a mesh size at each time step. Hence the search of the locations of the boundary cells is not time consuming.

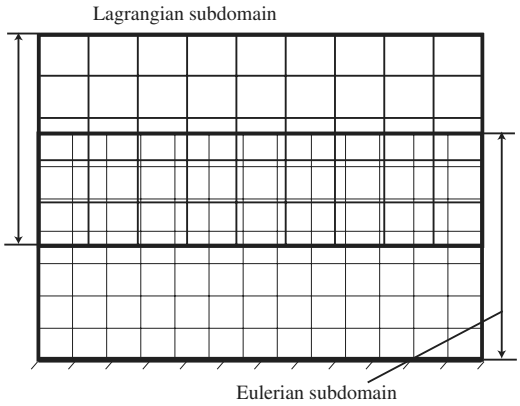

Fig. 4. Initial grid, there are several rows of grids in the overlapped region and the bottom of Lagrangian grid is far away for the boundary.

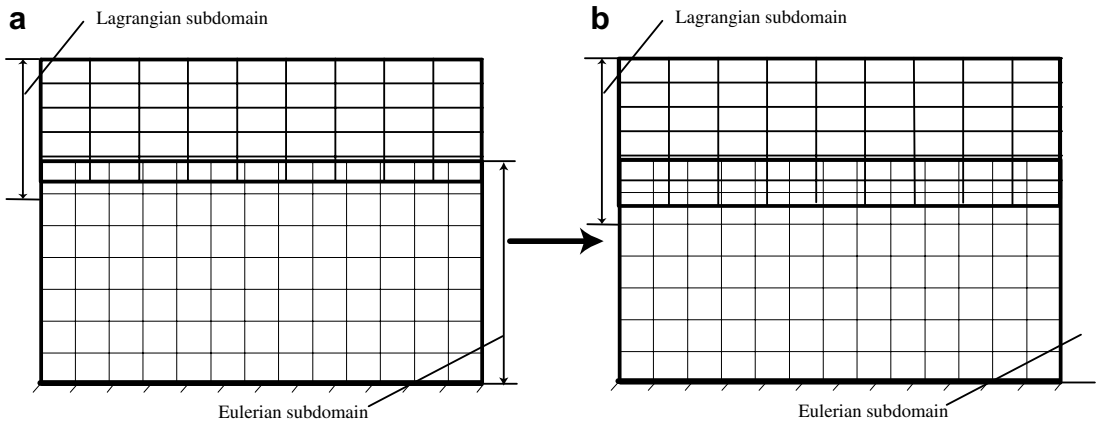

Fig. 5. The choice of Lagrangian grid in the overlapped region: (a) the Lagrangian grid moves away from the Euler subdomain; (b) a new row of the grid is generated automatically at the bottom of the Lagrangian subdomain.

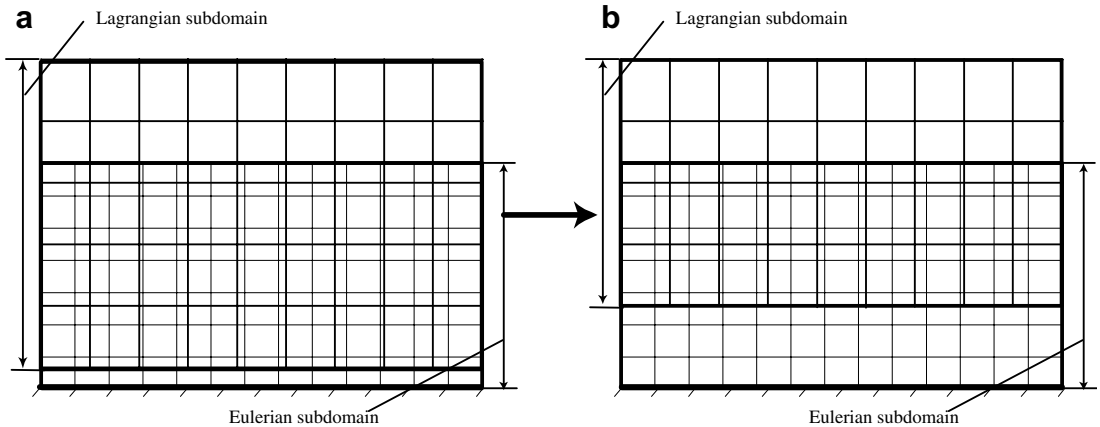

Fig. 6. The choice of Lagrangian grid closed to the boundary: (a) Lagrangian grid moves closer to the boundary; (b) the grid row in the Lagrangian subdomain nearest to the boundary is deleted automatically.

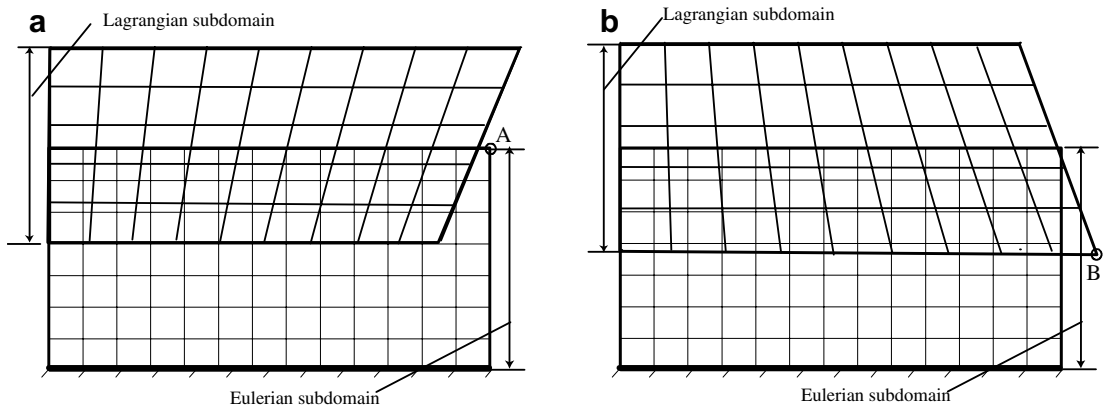

Fig. 7. The interface meshes are not overlapped by other cells: (a) the Lagrangian grid does not reach the initial right boundary; (b) the Lagrangian grid escapes the Euler subdomain.

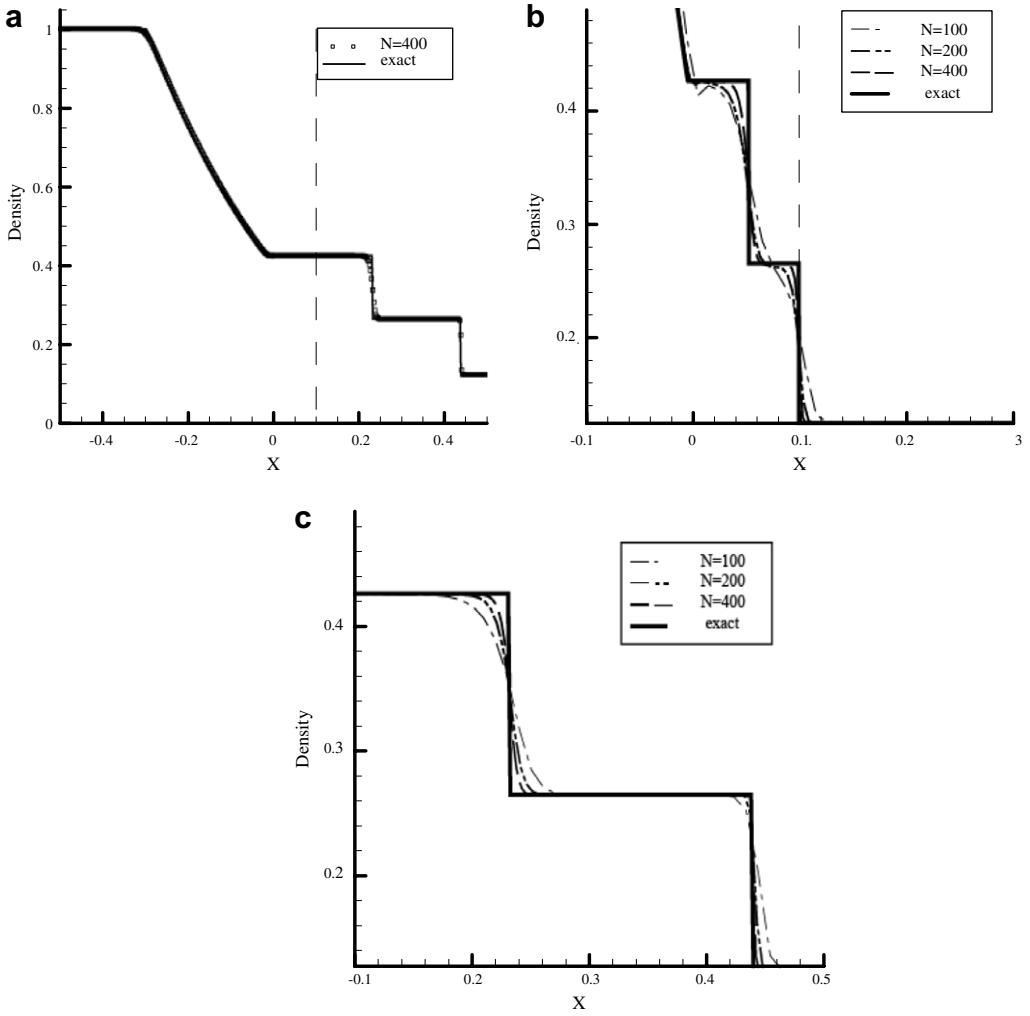

Fig. 8. The density distributions for 1D Riemann problem by the hybrid approach: (a) numerical solution with 400 cells at $t = 0.25$, compared with the exact solution; (b) numerical solution near the shock wave obtained with 100, 200, 400 cells at $t = 0.057$; (c) numerical solution near the shock wave obtained with 100, 200, 400 cells at $t = 0.25$.

Linear interpolation is used to define the interface conditions. For instance, the boundary condition at the cell center of "*abcd*" is defined by the bilinear interpolation

$$q(x,y) = a + bx + cy + dxy.$$

The coefficients a, b, c, d are obtained by putting

$$q_1(x_1,y_1) = a + bx_1 + cy_1 + dx_1y_1,$$
$$q_2(x_2,y_2) = a + bx_2 + cy_2 + dx_2y_2,$$
$$q_3(x_3,y_3) = a + bx_3 + cy_3 + dx_3y_3,$$
$$q_4(x_4,y_4) = a + bx_4 + cy_4 + dx_4y_4,$$

where q_1, q_2, q_3 and q_4 are the solutions at the center of the interior cells (of the Eulerian subdomain) $1,2,3,4$ of coordinates (x_1,y_1), (x_2,y_2), (x_3,y_3) and (x_4,y_4), respectively. The interface condition for the boundary cells of the Eulerian subdomain is similarly defined.

The new difficulties related to the hybrid approach, if they exist might arise from the interface. Interpolation at the interface due to noncoincidence of cell centers between the adjacent subdomains would induce instability and nonconservation. The stability and conservation for interface problems has been extensively studied in the past. Here we outline the main results which are concerned here.

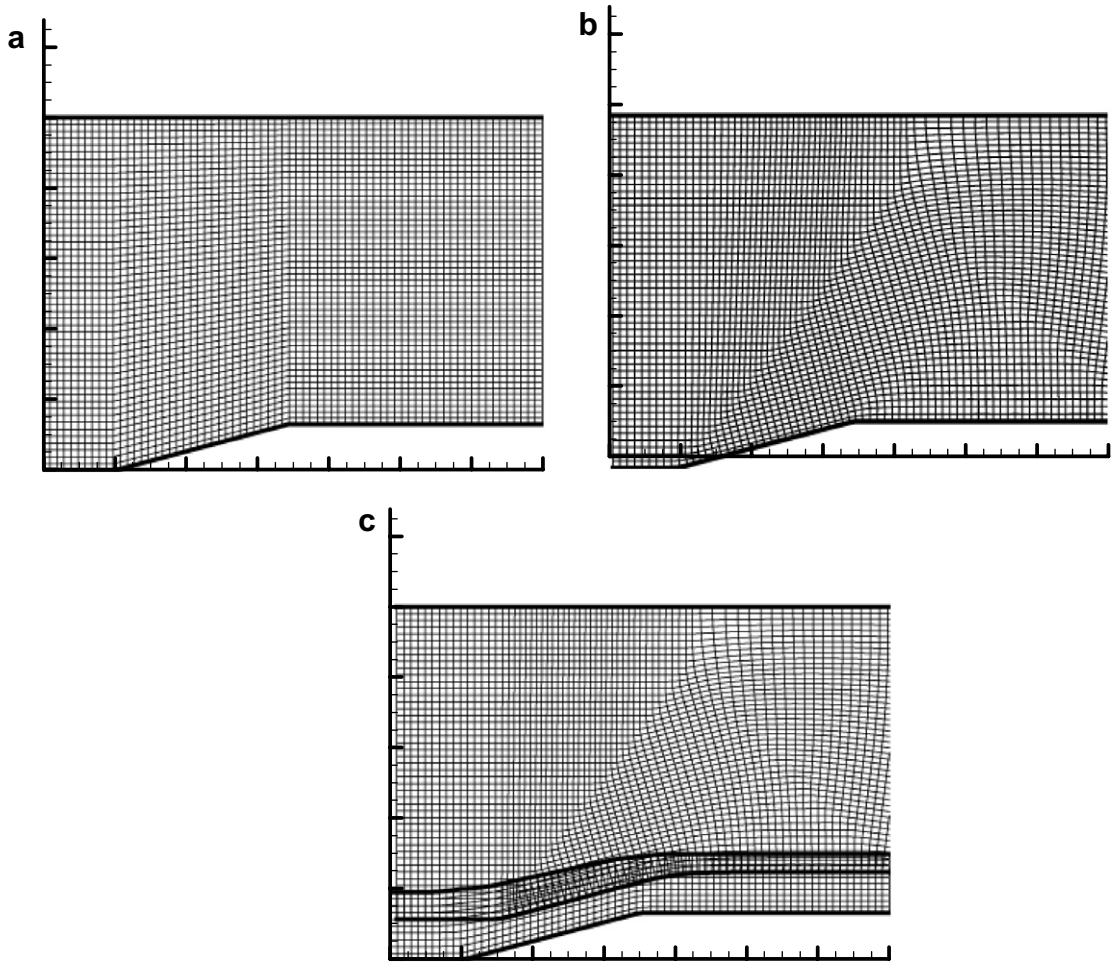

Fig. 9. Grid for Mach reflection problem: (a) Eulerian approach, (b) unified coordinate approach, (c) hybrid approach.

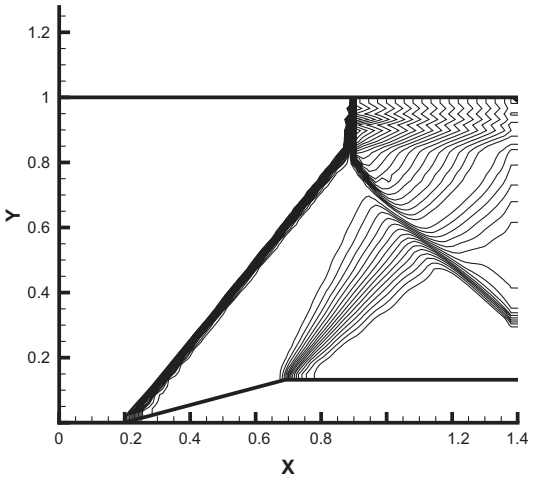
1.2
1
0.8
0.6
0.4
0.2
Y
0
0.2
0.4
0.6
0.8
1.2
1.4
X

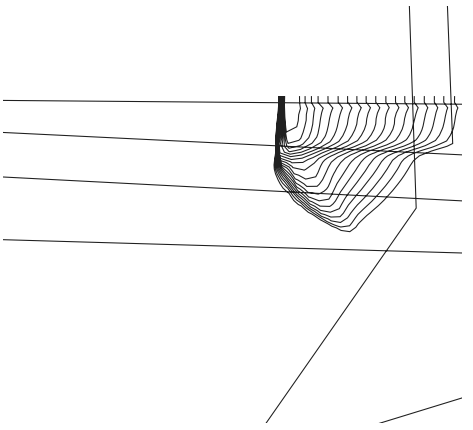

When the interior difference schemes are dissipative and three points in space, then using any normal interpolation formula with positive coefficients is stable [11,12]. For dissipative schemes with more than three points, stability can still be proven if there are enough mesh points in the overlap. Since we used normal interpolation here and the Godunov scheme that is dissipative, the hybrid approach is stable.

Conservation has been believed to be an important question. Berger [10] proposed to use flux interpolation to ensure conservation. However, this method was shown to be only weakly stable and is not suitable for steady state computation [13]. In [14,15], it was shown that conservation is important only for discontinuous waves, hence the real key point of conservation is whether a moving shock can transmit the overlapping grid interface without difficulties. The main conclusion is that using an interior scheme with enough numerical dissipation and using an interpolation like that given above ensures that the shock can transmit the interface correctly. In the present paper, we have used the Godunov scheme which contains sufficient numerical dissipation to satisfy the above requirement so that we do not encounter difficulties with conservation.

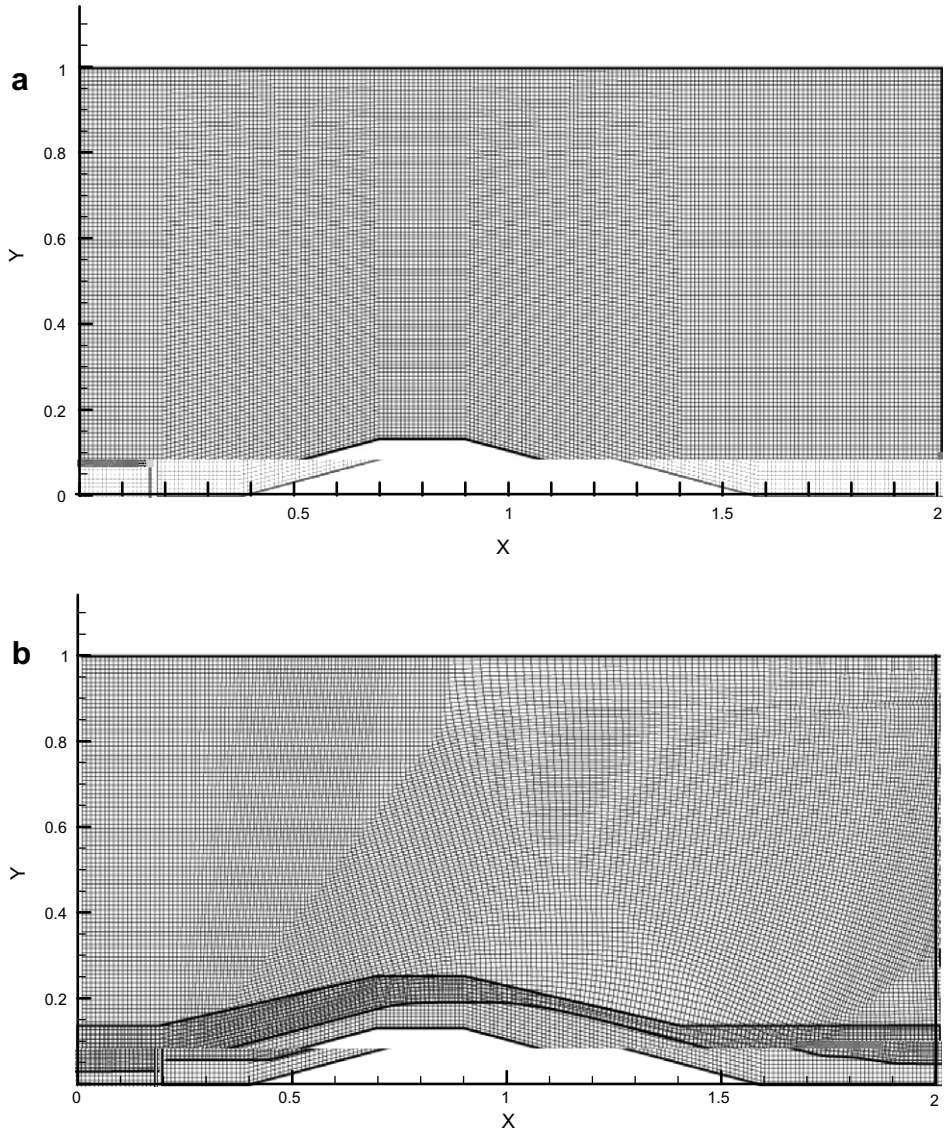

Fig. 12. Grid for Mach reflection problem with a 15° backward-facing step: (a) Eulerian approach; (b) hybrid approach.

meshes are not overlapped by other cells. Take the former case for example, the boundary conditions for Euler boundary cells are needed. Since the perturbation do not spread upstream in supersonic flows, the boundary conditions for Euler cells are defined by simple extrapolation of interior cell points, all gradients set to zero. Similarly, in the latter case, the boundary conditions for Lagrangian boundary cells are needed and simple extrapolation is used for the Lagrangian escaping cells.

3. Numerical experiments

In this section, the hybrid approach is tested numerically on four examples. $\gamma = 1.4$ is used in all the cases. The first test problem is a one-dimensional Riemann problem with grid refinement study to evaluate the accuracy of this hybrid technique. The second is a Mach reflection problem for inviscid flows, which is used to demonstrate that, in using the hybrid approach, we can avoid the influence of singular points while keeping the advantages in resolving discontinuities. The third is a shock/shock interaction problem for viscous flow, which is to show that the hybrid approach can handle a complex flow with shock waves, slip lines and boundary layers. The last example is a subsonic flow around an airfoil. In this example, we will demonstrate that the hybrid approach can also deal with subsonic flows.

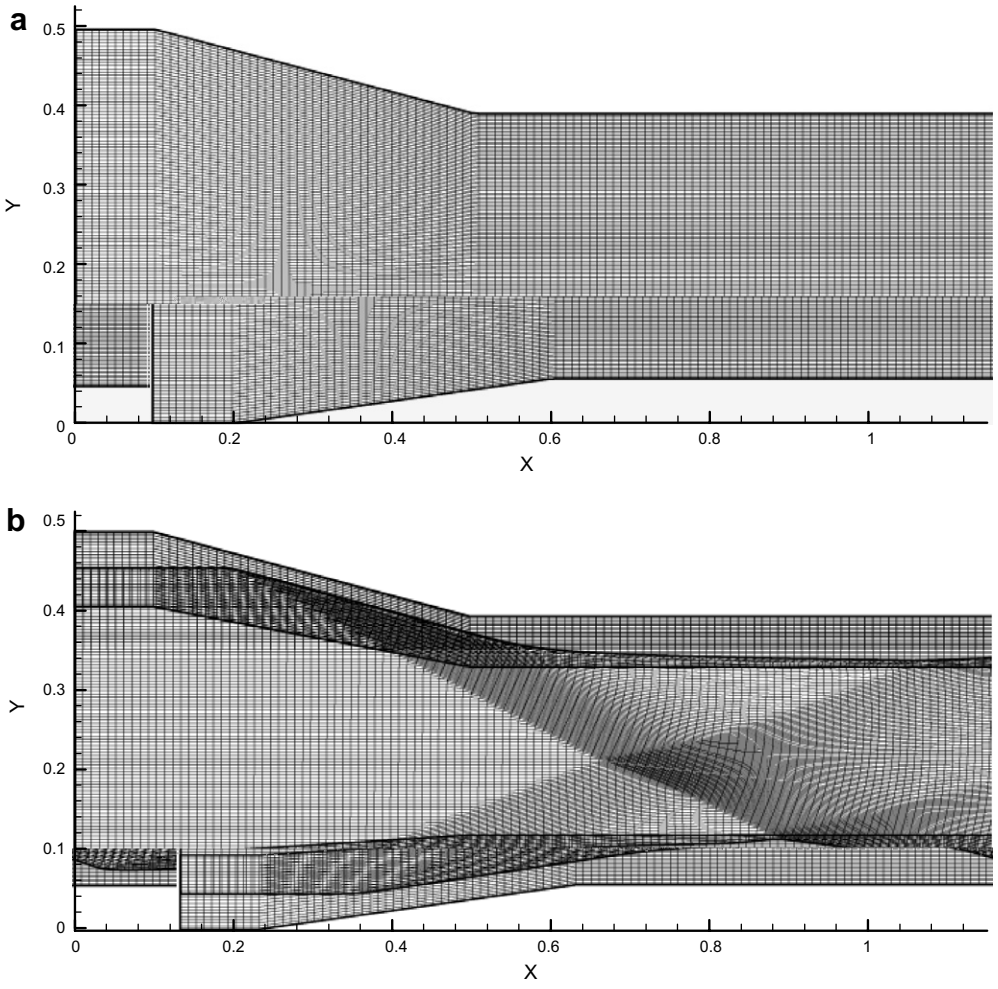

Fig. 14. Grid for shock interaction: (a) Eulerian approach; (b) hybrid approach.

Similarly as in [7], we use the Godunov method with the MUSCL update to higher resolution to solve the inviscid part of Navier–Stokes equations for viscous flows or Euler equations for inviscid flows. While the viscous part of Navier–Stokes equations will be discretized by using central differencing. Both types of subdomains use the same numerical scheme.

3.1. One-dimensional Riemann problem

The first example is a one-dimensional Riemann problem used to test the accuracy of this hybrid technique. The initial condition is

$$(\rho_l, u_l, p_l) = (1, 0, 1), \quad x \leqslant 0$$
$$(\rho_r, u_r, p_r) = (0.125, 0, 0.1), \quad x > 0.$$

The spatial domain is the interval $[-0.5, 0.5]$, which is divided into two subdomians. The left Eulerian coordinates subdomain is located between $[-0.5, 0.1]$ and the right unified coordinates subdomain is located between $[0.1, 0.5]$. In the course of computation, the unified coordinates are regenerated every time step. We ensure that the overlapped region between the two subdomains always has 3–4 cells.

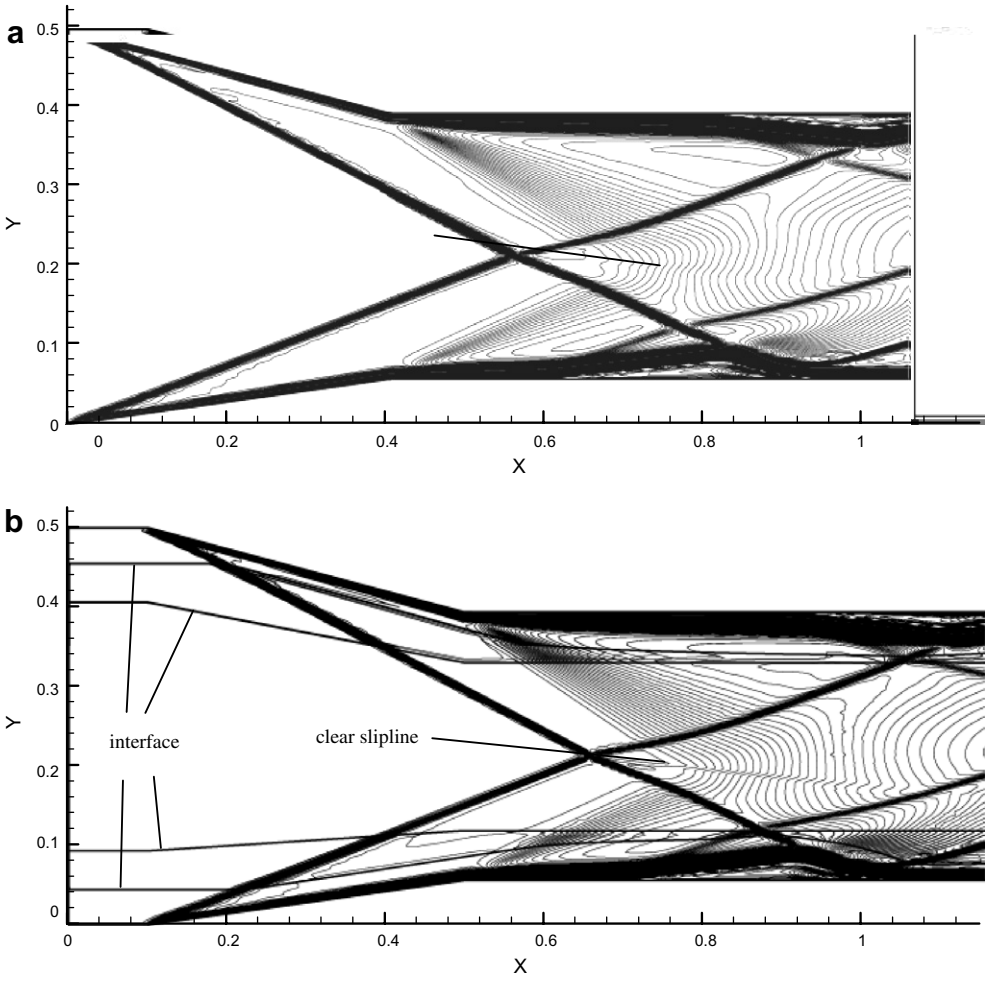

Fig. 15. Mach contours for shock interaction: (a) Eulerian approach; (b) hybrid approach.

The solution contains a left-going expansion wave, a contact discontinuity and a right-going shock. The expansion wave is always in the Eulerian coordinates subdomain. However, the contact discontinuity and the shock will cross the interface between the two subdomains.

In Fig. 8(a), we display the density distributions by the hybrid approach and the exact solution at $t = 0.25$. It is clear that the hybrid approach is very close to the exact solution. Fig. 8(b) displays the numerical solution near the shock wave obtained with different number of grid points for $t = 0.057$. At this instant the shock wave is close to the interface ($x = 0.1$). Fig. 8(c) displays the numerical solution near the shock wave at instant $t = 0.25$. At this instant the shock is far from the interface. From both Fig. 8(b) and (c), it is clear that with the grid refined, the numerical solution of the hybrid method approaches the exact solution.

3.2. Inviscid supersonic flow: Mach reflection problem

The second example is the Mach reflection of an inviscid flow from a wedge. A ramp of 15° is located between $x = 0.2$ and $x = 0.7$. The spatial domain is the interval $[0, 1.4] \times [0, 1]$. When an inviscid flow of $Ma = 1.8$ passes, an oblique shock, a Mach stem and a slip line are generated. The initial flow data are $(\rho, u, Ma) = (1, 1, 1.8)$ where Ma is the Mach number. The number of grid while using a pure Eulerian

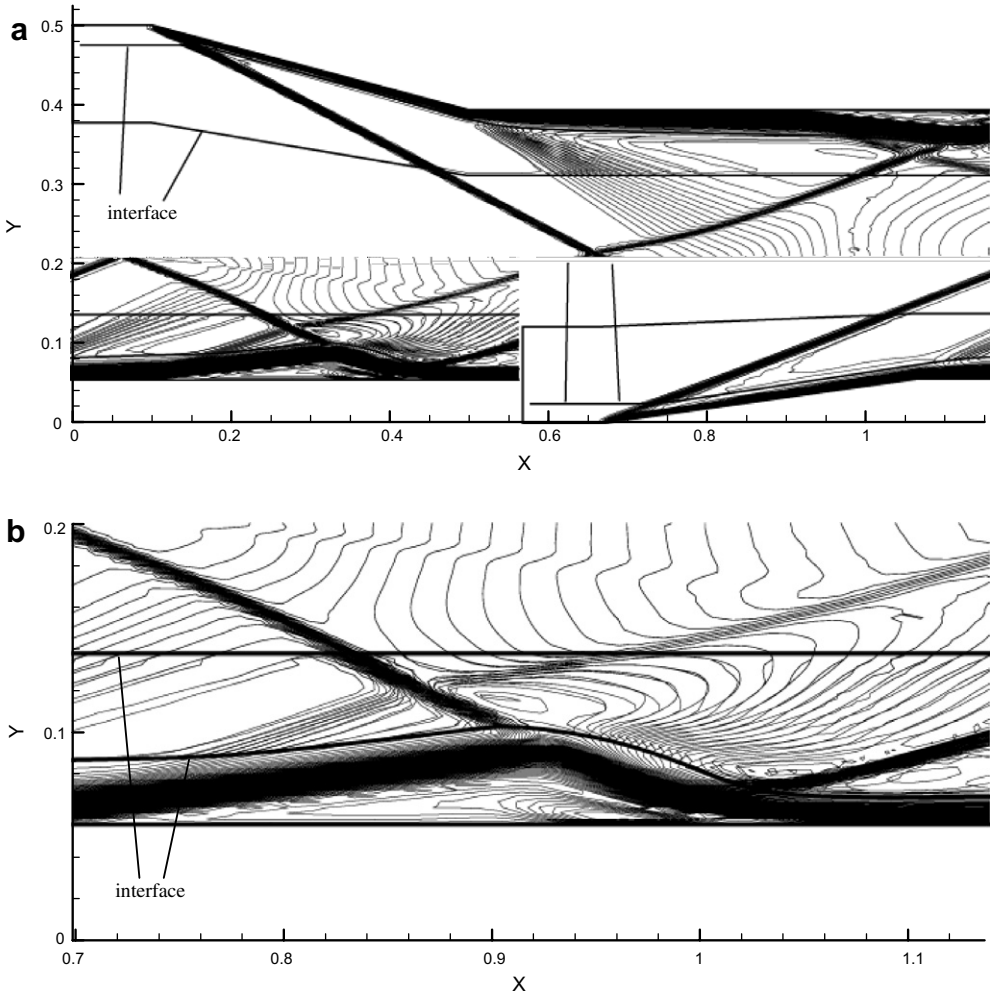

Fig. 16. Mach contours for shock interaction with the overlapping region enlarged: (a) the whole spatial domain; (b) close view of the intersection of shocks.

approach and a pure unified coordinate approach is 70×50. For the case of hybrid approach, the computational grid is 70×10 in the lower subdomain (Eulerian approach) and 70×44 in the unified coordinates subdomain.

Figs. 9 and 10 give the grid system and the Mach number contours using the Eulerian approach, the unified coordinates approach and the hybrid approach, respectively. By the pure Eulerian approach, the slip line from the triple point of Mach reflection is not well captured and the solutions is not quite smooth near the slip line (Fig. 10(a)). When the pure unified coordinate system is used, the slip line is well captured, but the flow around the ramp is not quite smooth (Fig. 10(b)). We can see clearly in Fig. 11, which is the local amplificatory figure of Fig. 10(b). This is due to the singularity effect and this effect contaminates the flow behind the reflected shock wave. The slip line is well resolved and the ramp region is smooth when the flow is computed with the hybrid approach (Fig. 10(c)).

A flow around an obstacle is also computed. This obstacle has a front ramp of 15° as for the previous example and a back ramp of 15°, located between $x = 0.9$ and $x = 1.4$. The spatial domain becomes $[0, 2.0] \times [0, 1]$. The number of grid using a pure Eulerian approach is 200×100. For the case of hybrid approach, the computational grid is 200×20 in the lower subdomain (Eulerian approach) and 200×90 in the unified coordinates subdomain.

Fig. 12(a) and (b) gives the grid system using the Eulerian approach and the hybrid approach. Fig. 13 gives the corresponding Mach contours. From Fig. 13(a), we can see that the solutions near the slip line are not quite smooth. Once again, the hybrid approach gives a better result (Fig. 13(b)).

3.3. Viscous supersonic flow: shock/shock interaction

The third example is a problem of shock/shock interaction. Two oblique shocks are generated by two wedges which cause a deflection of the flow by an angle $\theta = 8°$ (lower wedge) and $\theta = 15°$ (upper wedge). The upstream Mach number is $M_\infty = 4$. Viscous flow is considered. The Reynolds number is $Re = 10^5$. In using the Eulerian approach, the computational grid is 120×120. While in using the hybrid approach, the computational domain is decomposed into three subdomains. The two Eulerian subdomains are close to the lower wall and the upper wall, respectively. The middle is the unified coordinates subdomain. The computational grid is 120×15 and 120×110 in the Eulerian subdomain and in the unified coordinates subdomain, respectively. It has been shown that the use of a pure unified coordinate approach gives poor results for such a flow unless the grid near the wall is artificially fixed [9].

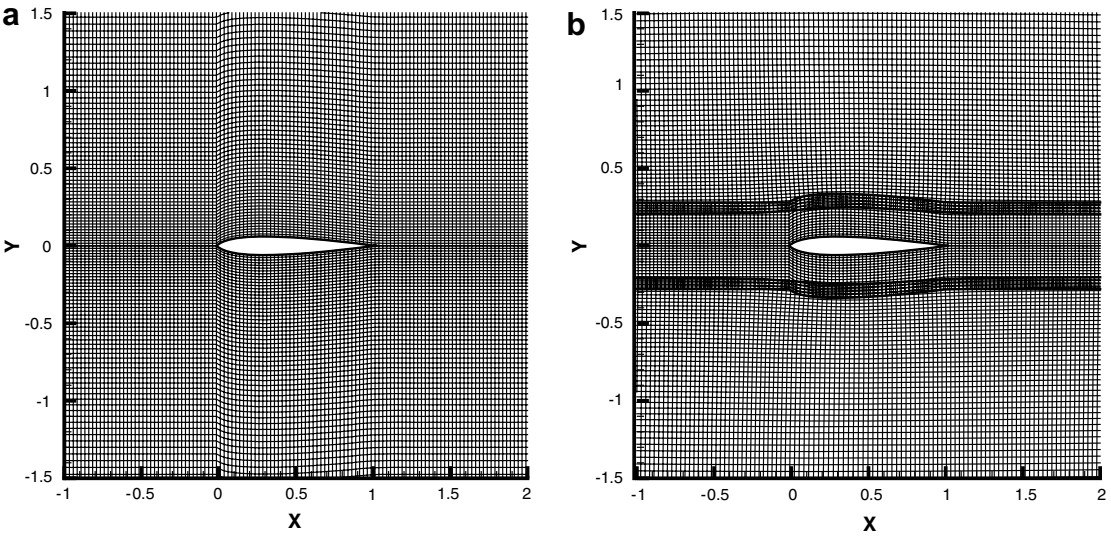

Fig. 17. Close view of mesh for flow past a NACA 0012 airfoil at zero angle of attack: (a) Eulerian approach; (b) hybrid approach.

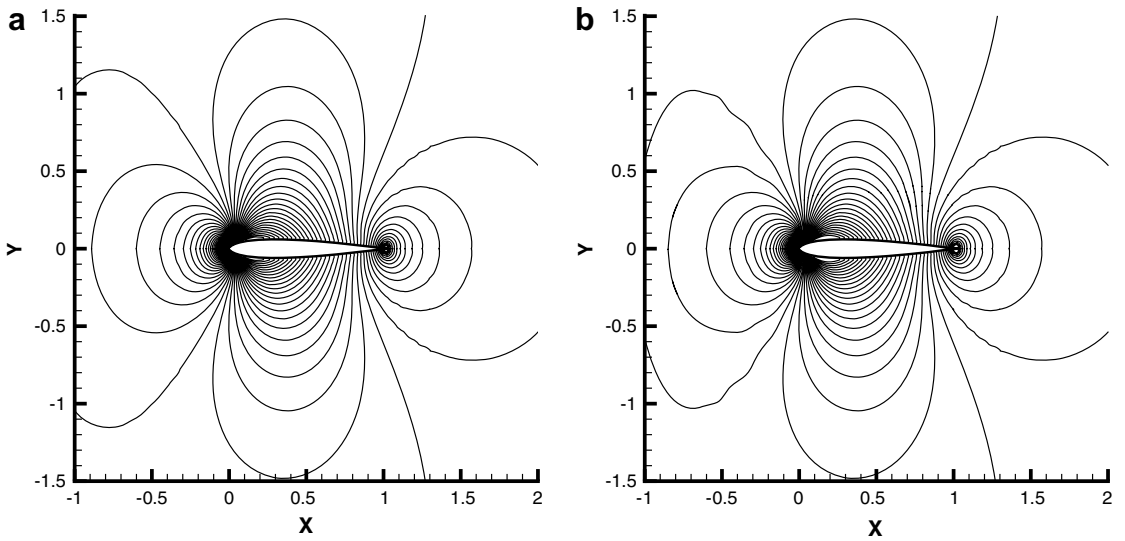

Fig. 18. Pressure contours for flow past a NACA 0012 airfoil at zero angle of attack: (a) Eulerian approach; (b) hybrid approach.

Fig. 14 gives the grid system for the Eulerian approach and the hybrid approach. As can be seen from Fig. 14(b), the grid automatically becomes denser near the shock. Fig. 15(a) shows the Mach contours obtained with the Eulerian approach. The numerical result is not accurate enough since the slip line between the two reflected shocks is not clearly captured. The numerical result is substantially improved by using the hybrid method. The Mach contours displayed in Fig. 15(b) contains a clear slip line. At the same time, it resolves the viscous features near the solid boundary without severe grid deformation.

In the case of Fig. 15, the shocks cross in the Lagrangian region. In order to see what happens when the intersection of shocks takes place inside the overlapping region, we make another computation where the overlapping region contains the intersection of shocks. The numerical results for the Mach contours are displayed in Fig. 16(a) and (b). From Fig. 16(b), we see that the shocks intersect in the overlapping region and pass through the interface smoothly.

3.4. Subsonic flow: flow around airfoil

Here we perform a computation for a compressible flow around an airfoil to show that this method also works for flows with an inflow Mach number less than 1.

The computational domain is decomposed into three subdomains. The middle Eulerian subdomain is close to the airfoil. The upper and the lower are the unified coordinate subdomains. The spatial domain is the interval $[-5,7]\times[-5,5]$ and the airfoil is located between $x=0$ and $x=1$. The computational grid is 480×30 in the Eulerian subdomain and 480×85 in each unified coordinate subdomain. The upstream Mach number is $M_\infty = 0.6$.

Fig. 17 shows close view of mesh near the airfoil with the Eulerian approach and the hybrid approach, respectively. Fig. 18 displays the corresponding pressure contours. From the above results, we see that the hybrid approach can also deal with subsonic flows.

4. Conclusions

Numerical experiments clearly demonstrate the advantages of using a hybrid Eulerian/Lagrangian approach for computing steady compressible flows with shock waves, slip lines and boundary layers: it resolves the slip line better than a pure Eulerian approach, while it can handle viscous boundary layer without severe grid deformation.

References

[1] J.L. Guermond, S. Huberson, W.Z. Shen, Simulation of 2D external viscous flows by means of a domain decomposition method, J. Comput. Phys. 108 (1993) 343–352.
[2] G.H. Cottet, P.D. Koumoutsakos, Vortex Methods: Theory and Practice, Cambridge University Press, 2000.
[3] A.J. Chorin, Numerical study of slightly viscous flow, J. Fluid Mech. 57 (1973) 785–796.
[4] R.P. Fedkiw, T. Aslam, S. Xu, The ghost fluid method for deflagration and detonation discontinuities, J. Comput. Phys. 154 (1999) 393–427.
[5] R.P. Fedkiw, T. Aslam, B. Merriman, S. Osher, A non-oscillatory Eulerian approach to interfaces in multimaterial flows, J. Comput. Phys. 152 (1999) 457–492.
[6] R.P. Fedkiw, Coupling an Eulerian fluid calculation to a Lagrangian solid calculation with the ghost fluid method, J. Comput. Phys. 175 (2002) 200–224.
[7] W.H. Hui, P.Y. Li, Z.W. Li, A unified coordinate system for solving the two-dimensional Euler equations, J. Comput. Phys. 153 (1999) 596–637.
[8] W.H. Hui, A. Koudriakov, A unified coordinate system for solving the three-dimensional Euler equations, J. Comput. Phys. 172 (2001) 235–260.
[9] W.H. Hui, Z.N. Wu, B. Gao, Preliminary extension of the unified coordinate system approach to computation of viscous flows, J. Sci. Comput. 30 (2) (2007) 301–344.
[10] M. Berger, On conservation at grid interfaces, SIAM J. Numer. Anal. 24 (1987) 967–983.
[11] E. Pärt-Enander, B. Sjögreen, Shock waves and overlapping grids, Uppsala University, Dept. of Scientific Computing, Report No. 131, January 1991.
[12] E. Pärt-Enander, B. Sjögreen, Conservative and non-conservative interpolation between overlapping grids for finite volume solutions of hyperbolic problems, Comput. Fluids 23 (1994) 551–574.
[13] Z.N. Wu, Uniqueness of steady state solutions for difference equations on overlapping grids, SIAM J. Numer. Anal. 33 (1996) 1336–1357.
[14] Z.N. Wu, Steady and unsteady shock waves on overlapping grids, SIAM J. Sci. Comput. 20 (1999) 1850–1874.
[15] Z.N. Wu, Transmission of a slowly moving shock across a nonconservative interface, J. Comput. Phys. 171 (2) (2001) 579–615.